Islamic Azad University

Journal of

Optoelectronical Nanostructures

Winter 2024 / Vol. , No.

Research Paper

Modeling Graphene-based PIN-FET with Quantum Dot Channel

Karim Milanchian[1], Hakimeh Mohammadpour*[,2]

[1] Department of Physics, Payame Noor University, Tehran, Iran.
[2] Department of Physics, Faculty of Basic Sciences, Azarbaijan Shahid Madani University, 53714-161 Tabriz, Iran

Received: 4 Oct. 2023
Revised: 18 Nov. 2023
Accepted: 5 Dec. 2023
Published: 15 Dec. 2023

Use your device to scan and read the article online

Keywords:
FET, Graphene, NEGF, Quantum Dot

Abstract:
Discrete energy levels of quantum dots (QD) have electronic and optoelectronic applications. In this paper, a novel graphene nanoribbon (GNR) field effect transistor (FET) is modeled numerically using the NEGF formalism. In the new device model of this paper, the channel region is composed of one or two QDs, made by only one metallic gate electrode. This model utilizes a semiconductor armchair graphene nanoribbon through which the current may pass. The two highly doped ends of GNR act as source and drain contacts. At this unique model, one or two quantum dots form on GNR channel. The discreteness of energy levels of the two coupled quantum dots, revealed by applying gate voltage, gives rise to resonant tunneling. Resonant tunneling through these levels results in negative differential conductance. The coupling between QDs determines the current characteristics of device. Step-wise increment of current by increasing drain voltage manifests QDs discrete energy levels.

Citation: Karim Milanchian, Hakimeh Mohammadpour. Modeling Graphene-based PIN-FET with Quantum Dot Channel. **Journal of Optoelectronical Nanostructures. 2023; 8 (4): 82- 96** . DOI: **10.30495/JOPN.2024.32047.1292**

***Corresponding author:** Hakimeh Mohammadpour
Address: Department of Physics, Azarbaijan Shahid Madani University, Tabriz, Iran.
Tell: 009891440764017302 7100 **Email:** sa_zaras@yahoo.com

1. INTRODUCTION

Discrete energy levels of quantum dots (QD) have electronic and optoelectronic applications [1-5]. Phototransistors, which are FETs with light detection ability, are among the modern devices which functionality is based on the discrete energy levels of the device [6-8]. This discreteness may give rise to negative differential resistance (NDR) which has many applications in today's fast electronics [9-20].

Two-dimensional flat structure of graphene and its carrier's ballistic transport of very high mobility, leads to applications of graphene-based QDs in quantum devices. GNR-phototransistors with discrete density of states, provide optical response spectra with sharp peaks. The discrete energy levels of QD may also give rise to resonant tunneling and NDR. In ref. [2], QD-channel on graphene FET is modeled by different engineering method on GFET.

In the new device model of this paper, the channel region is composed of one or two QDs, made by only one metallic gate electrode. In the next section, the structure and working essentials of the new GFET are explained. If one incorporates the spin of electrons e.g. by using ferromagnetic substrate, spintronic applications are allowed. QDs spin valves have applications in the spin injection and detection processes [21-23]. QDs are possible candidate elements in quantum computers [24-27].

2. GFET MODEL

Diagram of the modeled device is plot schematically in Fig. 1. It manifests a Metal-Oxide-Semiconductor field effect transistor with GNR channel and a modified gate contact. This construction creates a couple of quantum dots (QD) at the channel of device. The current-carrying QDs and the source and drain electrodes are designed on semiconducting armchair graphene nanoribbon (A-GNR) of 1.5 nm width that has band gap of about 0.72eV. By heavily doping the two ends of GNR, the source and drain contacts with high density of states are constructed. This GNR, is layed between two SiO2 layers (dielectric constant k = 3.9) having thickness of 0.8 nm.

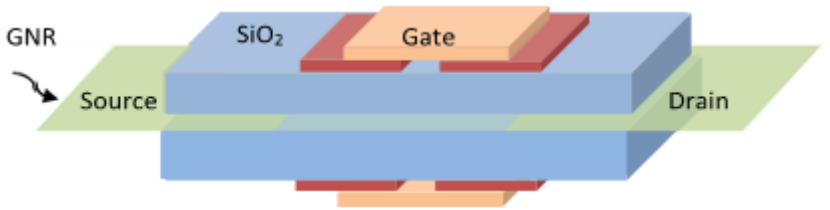

Fig. 1. Schematic diagram of coupled QD GNR-FET.

The GNR-FET (GFET) structure has symmetry on top and bottom about the GNR layer.

The new structure introduced is a new configuration of GNR-based PIN-FET (Field effect transistor with p-type source and n-type drain doping) with unique geometry of gate electrode that forms quantum dots in channel.

In the model, drawn schematically in Fig. 1, two metallic plates cover the dielectric layer on top of channel regions. Another metallic electrode also lay on top of the two plates. By this construction, the plates are equipotential while the gate voltage is connected. Therefore, by this arrangement, by applying gate voltage, in the GNR channel a barrier forms between the two metallic plates. In order to construct barriers between the channel and the contacts (source and drain) two possibilities are employed. For designing the source-connected barrier, p-type source doping is adopted so that the doping type of the source and n-type QD-channel are different. For designing the drain-connected barrier, the gate plate, does not cover a thin layer (we chose four unit cells) of channel in contact to the highly doped drain contact and so, it is not under the gate control and acts as barrier.

This model structure for GFET (Fig. 1), creates two separate n-type conducting QD channels with discrete energy levels by applying gate voltage. A thin barrier couples these QDs to each other. Discrete energy levels are constructed at the channel and contribute to the resonant tunnelling of electrons.

The potential energy profile, charge density and current are determined by solving Poisson equation and the non-equilibrium Green's function (NEGF) equations [28]. NEGF is used for real-space tight-binding Hamiltonian (H) for GNR (by hopping energy t = 2.7eV) [29].

The Green's function is

$$G(E)=[(E+i\eta)I-H-U-\sum_{s}-\sum_{d}]^{-1} \quad (1)$$

E is energy and U is a diagonal matrix with on-site potential energies. The source- and drain-connected self-energies are Σ_s and Σ_d [30] and η is a small number.

$$\Sigma_{d(s)} = \tau g_{R(L)} \tau^{\dagger}, \quad g_{R(L)} = [(E + i\eta) I - H_{R(L)}]^{-1} \tag{2}$$

$H_{R(L)}$ and $g_{R(L)}$ are the Hamiltonian and Green's functions of the right (left) contact, respectively. The iterative algorithm of ref. [30] calculates the self-energies. The energy level broadenings of channel by the source and drain contacts are, $\Gamma_{s(d)} = i(\sum_{s(d)} - \sum_{s(d)}^{\dagger})$

The potential energy, U, in Eq. (1) is obtained by solving Poisson equation (4) at the whole simulated device;

$$\vec{\nabla}.\left(\varepsilon \vec{\nabla} U\right) = e^2 n \tag{3}$$

The electron density is calculated from the NEGF formalism,

$$n = 2\int_{-\infty}^{+\infty} \frac{dE}{2\pi} G^n(E) \tag{4}$$

G^n, the electron correlation function is determined from

$$G^n = G \Sigma^{in} G^{\dagger} \tag{5}$$

where Σ^{in}, is defined

$$\Sigma^{in}(E) = \Gamma_s(E) f_s(E, E_{Fs}) + \Gamma_d(E) f_d(E, E_{Fd}) \tag{6}$$

$f_{s(d)}\left(E, E_{Fs(d)}\right)$ is the source (drain) Fermi-Dirac distribution function.

In order to obtain the device current in the ballistic regime, Landauer formula is employed as,

$$I = \frac{2e}{\hbar} \int_{-\infty}^{+\infty} dE T(E) \left(f_s(E) - f_d(E) \right) \tag{7}$$

In this formula, T(E) is the electronic transmission function at energy E. According to this equation, mainly the states at energy intervals between the source and the drain Fermi levels contribute to the current.

In the NEGF formalism, T(E) is;

$$T(E) = Tr\left[\Gamma_s G \Gamma_d G^{\dagger}\right] \quad (8)$$

3. RESULTS AND DISCUSSION

The lengths are attributed to the number of unit cells along the ribbon length. Each unit cell of an AGNR is a rectangle of a width equal to that of a Benzene ring and the length of all Benzene rings along the width of ribbon. Therefore, it is assumed that the ribbon is a one-dimensional structure. The width of unit cells, is about 0.43 nm and the length is about 1.5 nm.
The channel length, N_{Ch}, contains the lengths of the dots, N_{D1}, N_{D2}, the barrier between dots, $N_{B\text{-in}}$, and the channel to drain barrier, $N_{B\text{-out}}$. We fix the latter at 4 (unit cells). Therefore, $N_{Ch} = N_{D1} + N_{B\text{-in}} + N_{D2} + 4$. If we set the barrier width, N_B equal to zero, single QD forms in channel.

A. Single QD-GFET

The first set of parameters are related to a single QD-FET using the channel parameters: $N_D = 20$, $N_{B\text{-out}} = 4$. The conduction and valence bands are shown in Fig. 2 for V_D=0.2V and V_G equal to 0.8V and 1.2V. As expected from the designed structure, two barriers form at the interface between channel and source and drain. Therefore, a QD forms in the channel.

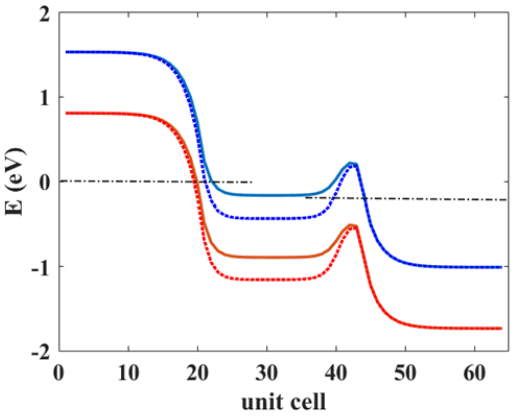

Fig. 2. Conduction (blue) and valence (red) bands along channel for V_D = 0.2V and V_G=0.8V (solid), 1.2V (dot).

In Fig. 3 the device $I - V_D$ characteristic curves are plot for different gate voltages, V_G. An increase of current by the drain voltage in step-like manner is revealed. This is a manifestation of the discreteness of energy levels in QD channel. As indicated by arrows for first steps, the step edge that stands for one of the energy levels shifts along drain voltage axis. This is due to the shift of energy levels of QD by changing the depth of QD by applying the gate voltage. The following section, in which we consider double-QD channel, provides more diagrams with detailed explanations.

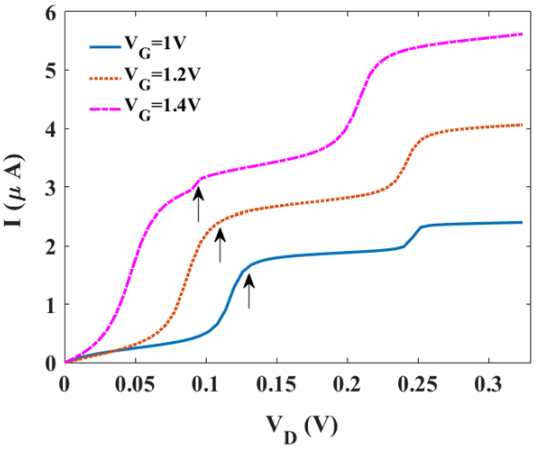

Fig. 3: $I - V_D$ curves for N_D = 20 and different amounts of V_G.

B. DOUBLE QD-GFET

The set of parameters of a double QD-FET are N_{D1} = 24, N_{D2} = 15, $N_{B\text{-in}}$ =6 and $N_{B\text{-out}}$ = 4.
The conduction and valence bands are shown in Fig. 4 for V_D=0V and V_G=1.4V. At this structure, there are two barriers at the two ends of channel and a barrier inside the channel. Therefore, two QDs form in series at the channel.

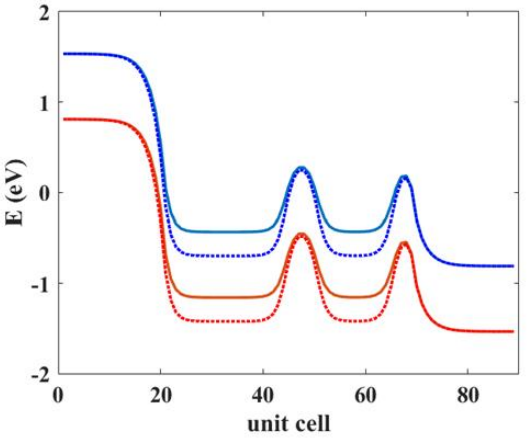

Fig. 4: Conduction (blue) and valence (red) bands for V_G=1.2V (solid), 1.6V (dot).

The density of electrons (LDE) in the channel is present in Fig. 5 for V_G=1.6V and V_D=0.3V. The energy levels of QDs and the edge of the conduction band are observed. In addition, the energy modes of electrons in the left QD manifest decreasing wavelength by increasing energy.

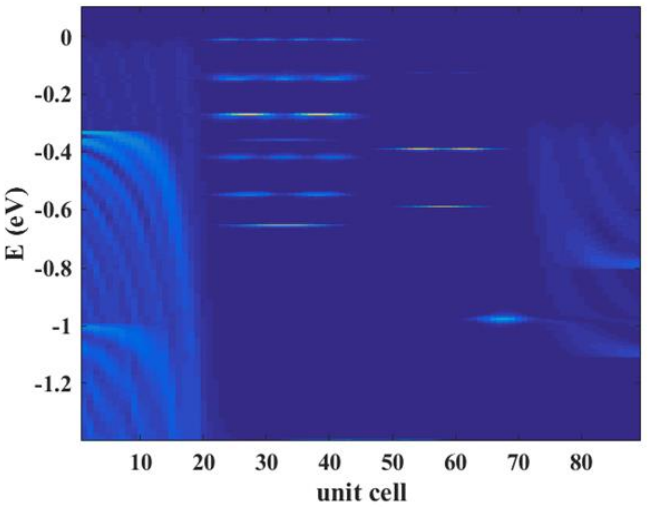

Fig. 5: Color plot of DOE along channel.

Since the two QDs have different widths, they have different distributions of discrete energy levels. Therefore, current of the channel is carried through the aligned energy levels of the two QDs.
The $I-V_D$ characteristic curves of device are plot in figure 6 for different amounts of V_G.

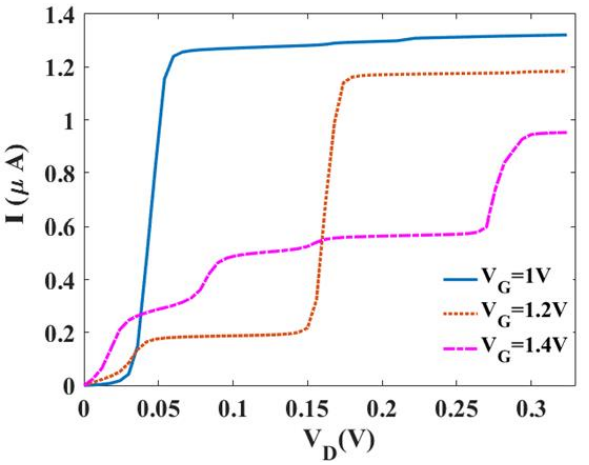

Fig. 6: $I-V_D$ characteristics for different amounts of V_G.

We observe that in contrast to normal GFETs, current does not necessarily increase by increasing the gate voltage, V_G. This is a footprint of quantum effect of confinement. By increasing the QD depth by the gate voltage, the energy level distribution changes. This may result in two significant effects: 1- some energy levels which contributed to the current, may shift to the outside of the current-related energy window (the energies between source and drain Fermi energies) and 2- some energy levels of the two QDs which were aligned at some gate voltage, will lose alignment.
To investigate current behavior by changing the gate voltage, we plot the current curve versus gate voltage, $I - V_G$ in figure 7 for double-QD FET.

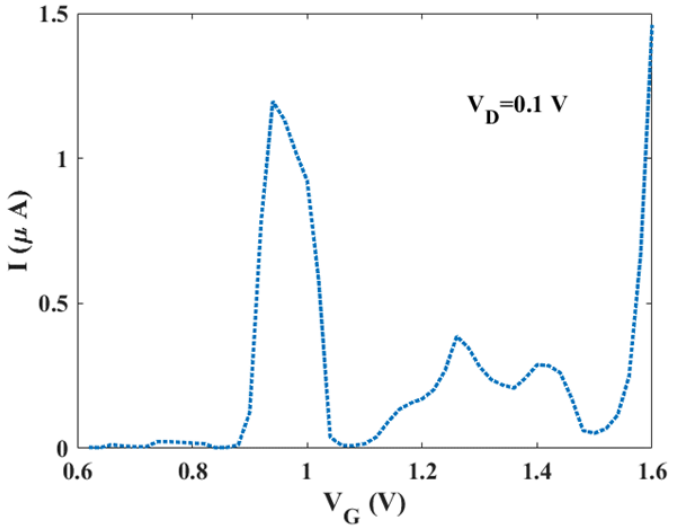

Fig. 7: $I - V_G$ curve for V_D=0.1V.

The current oscillation by the gate voltage results in negative differential conductance.

4. CONCLUSIONS

We introduce a new design for GFET model with p|i|n doping structure. Unlike traditional GFETs the gate metal governs the electrostatics of two distinct regions of the GNR channel. Also a quantum barrier separates two regions of the channel while two other barriers forms between source and drain reservoirs and the channel. This quantum confinement by the barriers gives rise to formation of quantum dots and discrete energy levels in the channel. Current increases in step-like manner by increasing the drain voltage. This behaviour of the device current has applications in nanoelectronics, optoelectronics and quantum computing.

ACKNOWLEDGMENT

This research was supported by Azarbaijan Shahid Madani University.

REFERENCES

[1] K. Hasanirokh, A Asgari and S Mohammadi, *Infrared navigation—Part I: An assessment of feasibility*, Journal of the European Optical Society-Rapid Publications, 17 (Dec. 2021) 1-10.
Available:https://jeos.springeropen.com/articles/10.1186/s41476-021-00173-8

[2] H. Mohammadpour, *Quantum dot resonant tunneling FET on graphene*, Physica E, 81 (Jul. 2016) 91.
Available:https://www.sciencedirect.com/science/article/abs/pii/S1386947716300649

[3] D. Ghosh, K. Sarkar K, P. Devi P, K. H. Kim and P. Kumar, *Current and future perspectives of carbon and graphene quantum dots: From synthesis to strategy for building optoelectronic and energy devices*, Renewable and Sustainable Energy Reviews, 135 (Jan. 2021) 110391.

Available:https://www.sciencedirect.com/science/article/abs/pii/S1364032120306791

[4] X. Shi, X. Liu and H. Zeng, *ZrO2 quantum dots/graphene phototransistors for deep UV detection*, Materials Research Bulletin, 96 (Dec. 2017) 458-462.
Available:https://www.sciencedirect.com/science/article/abs/pii/S002554081731334X

[5] H Agarwal et al *Engineering Negative Differential Resistance in NCFETs for Analog Applications*, IEEE Transactions on Electron Devices, 68 (May 2018) 2033-2039.
Available: https://ieeexplore.ieee.org/document/8331968

[6] I. Nikitskiy, S. Goossens, D. Kufer, T. Lasanta, G. Navickaite, F. H. L. Koppens & G. Konstantatos, *Integrating an electrically active colloidal quantum dot photodiode with a graphene phototransistor*, Nat. Commun., 7 (Jun. 2016) 11954.
Available: https://www.nature.com/articles/ncomms11954

[7] V. Ryzhii, *The theory of quantum-dot infrared phototransistors*, Semiconductor Science and Technology, 11 (Jan. 1996) 759.
Available: https://iopscience.iop.org/article/10.1088/0268-1242/11/5/018

[8] G. Konstantatos, M. Badioli, L. Gaudreau Gerasimos, J. Osmond, M. Bernechea, F. Pelayo G. Arquer, F. Gatti & F. H. L. Koppens. *Hybrid graphene–quantum dot phototransistors with ultrahigh gain*. Nature Nanotech,7(2012, May.) 363–368.
Available: https://www.nature.com/articles/nnano.2012.60

[9] M. Akbari Eshkalak, R. Faez. *A computational study on the performance of Graphene Nanoribbon Field Effect Transistor*. Journal of Optoelectronical Nano Structures, 2(3) (2017, Aug.) 1-12.
Available: https://jopn.marvdasht.iau.ir/article_2427.html

[10] Z. Rohani, A. A. Emrani Zarandi. *Designing a novel high-speed ternary-logic multiplier using GNRFRT technology*. Journal of Optoelectronical Nano Structures, 8(1) (2023, Jan.) 1-12.

Available: https://jopn.marvdasht.iau.ir/article_5800.html

[11] M. Rahimian. *Controlling ambipolar current in a junctionless Tunneling FET emphasizing on depletion region extension*. Journal of Optoelectronical Nano Structures, 8(1) (2023, Jan.) 13-31. Available: https://jopn.marvdasht.iau.ir/article_5899.html

[12] V. Khademhosseini, D. Dideban and M. Ahmadi. *Current Analysis of Single Electron Transistor Based on Graphene Double Quantum Dots*. ECS Journal of Solid State Science and Technology,9(2020, Jan.) 021003. Available: https://iopscience.iop.org/article/10.1149/2162-8777/ab6980

[13] H. Mohammadpour, Double Quantum Dot FET on graphene. JETP Letters, 114 (11) (2021 Nov.) 707-712. Available:https://link.springer.com/article/10.1134/S002136402123003X

[14] S. Afshari, J. Jahanbin Sardroodi, H. Mohammadpour, Electronic Behavior of Doped Graphene Nanoribbon Device: NEGF+DFT. Journal of Nanoanalysis, 4(4) (2017, Sept.) 272-279. Available:https://jnanoanalysis.tms.iau.ir/article_539940.html

[15] S. Salimpour, H. Rasooli Saghai, Impressive Reduction of Dark Current in InSb Infrared Photodetector to achieve High Temperature Performance. Journal of Optoelectronical Nano Structures, 3(4) (2018, Oct.) 81-96. Available:https://jopn.marvdasht.iau.ir/article_3265_698c93521a209e8daff27bb7ec5f43d5.pdf

[16] S. Ghajarpour-Nobandegani, M. J. Karimi, H. Rahimi, Tunable Terahertz Absorber Based on Graphene Disk Array. Journal of Optoelectronical Nano Structures, 8(2) (2023, May) 1-14. Available:https://jopn.marvdasht.iau.ir/article_5921.html

[17] M. Jabbari, M. Dehghan, M. K. Moravvej Farshi, G. Darvish, M. Ghaffari-miab. Ultra-Compact Bidirectional Terahertz Switch Based on Resonance in Graphene Ring and Plate. Journal of Optoelectronical

Nano Structures, 4(4) (2019, Dec.) 99-112. Available:https://jopn.marvdasht.iau.ir/article_3761_d2fa3599c18c16e0315c6611e3236684.pdf

[18] M. Riahinasab, E. Darabi. Analytical Investigation of Frequency Behavior in Tunnel Injection Quantum Dot VCSEL. Journal of Optoelectronical Nano Structures, 3(2) (2018, Jun.) 65-86. Available:https://jopn.marvdasht.iau.ir/article_2876_3ac61163b777771c8c771cc5f808bb45.pdf

[19] F. Hakimian, M. R. Shayesteh, M. Moslemi. A Proposal for a New Method of Modeling of the Quantum Dot Semiconductor Optical Amplifiers. Journal of Optoelectronical Nano Structures, 4(3) (2019, Aug.) 1-16. Available:https://jopn.marvdasht.iau.ir/article_3616_eb2f17e255bbbe8e99a32629674ad938.pdf

[20] M. Rezvani Jalal, M. Habibi, Simulation of Direct Pumping of Quantum Dots in a Quantum Dot Laser. Journal of Optoelectronical Nano Structures, 2(3) (2017, May) 61-70. Available:https://jopn.marvdasht.iau.ir/article_2425_968b2c48351292f237924ada4af47699.pdf

[21] P Tulewicz, K Wrześniewski and I Weymann. *Spintronic transport through a double quantum dot-based spin valve with noncollinear magnetizations*. Journal of Magnetism and Magnetic Materials,546(2022, Mar.) 168788. Available: https://www.sciencedirect.com/science/article/abs/pii/S0304885321010118

[22] A Bordoloi, V Zannier, L Sorba, C Schönenberger and A Baumgartner. *A double quantum dot spin valve*. Communications Physics 3(2020, Jan.) 135. Available: https://www.nature.com/articles/s42005-020-00405-2

[23] T. Ghaffary, F. Rahimi, Y. Naimi, H. Khajeazad, *Study of the spin-orbit interaction effectson energy levels and the absorption coefficients of spherical quantum dot and quantum antidote under the magnetic field.* Journal of Optoelectronical Nano Structures, 6(2) (2021, May) 55-74. Available: https://jopn.marvdasht.iau.ir/article_4769.html

[24] L Gyongyosi, S Imre S. *A Survey on quantum computing technology*. Computer Science Review 31(2019, Feb.) 51-71. Available: https://www.sciencedirect.com/science/article/abs/pii/S1574013718301709

[25] M. R. Mohebbifar. *Study of the Purcell factor of a single photon source based on quantum dot nanostructure for quantum computing applications.* Journal of Optoelectronical Nano Structures, 6(4) (2021, Oct.) 95-108. Available: https://jopn.marvdasht.iau.ir/article_5052.html

[26] M. Amirhoseiny, G. Alahyarizadeh. Enhancement of Deep Violet InGaN Double Quantum Wells Laser Diodes Performance Characteristics Using Superlattice Last Quantum Barrier. Journal of Optoelectronical Nano Structures, 6(2) (2021, May) 107-120. Available:https://jopn.marvdasht.iau.ir/article_4776_4941a2547e09c61dfc979b5fed25a722.pdf

[27] A. Asrar, M. Servatkhah, M. Yasrebi. Providing a Bird Swarm Algorithm based on Classical Conditioning Learning Behavior and Comparing this Algorithm with sinDE, JOA, NPSO and D-PSO-C Based on Using in Nanoscience. Journal of Optoelectronical Nano Structures, 5(3) (2020, Aug.) 39-58. Available:https://jopn.marvdasht.iau.ir/article_4403_36539ec52741c9b9bd4c97d2445d2d1e.pdf

[28] S Datta. *Quantum Transport: Atom to Transistor*. New York: Cambridge University Press, 2005, 183-249.

[29] K. I. Bolotin, K. J. Sikes, Z. Zhang, M. Klima, G. Fudenberg , J. Hone, P. Kim , H.L. Stormer . *Ultrahigh electron mobility in suspended graphene*. Solid State Commun. 3(2008, Jun.) 351-355. Available: https://www.sciencedirect.com/science/article/abs/pii/S0038109808001178

[30] R Lake, G Klimeck, R C Bowen and D Jovanovic*Single and Multiband Modeling of Quantum Electron Transport Through Layered Semiconductor Devices*. Journal of Applied Physics 81(1997, Feb.) 7845-7869.
Available:https://pubs.aip.org/aip/jap/article-abstract/81/12/7845/492121/Single-and-multiband-modeling-of-quantum-electron?redirectedFrom=fulltext